ELSEVIER

Catalysis Today 48 (1999) 147–159

CATALYSIS TODAY

Dynamics of internal diffusion during the hydrogenation of 1,5,9-cyclododecatriene on Pd/Al_2O_3

C. Julcour, J.M. Le Lann, A.M. Wilhelm, H. Delmas*

Laboratoire de Génie Chimique, CNRS ENSIGC/INPT, 18 Chemin de la Loge, 31078 Toulouse Cedex, France

Abstract

Dynamic and pseudo-steady state diffusion–reaction models were simulated for the three-phase consecutive hydrogenation of 1,5,9-cyclododecatriene on a shell Pd/Al_2O_3 catalyst in order to examine the time evolution of concentration profiles inside the catalyst pellet: a model accounting only for the dynamics of the active layer and a model taking also into account the inert part of the catalyst were compared.

In the conditions of the semibatch experiments (T=433 K, p_{H_2}=1.2 MPa), all the models lead to the same bulk concentration–time curves, but the hydrocarbon concentration profiles in the pores are dependent on the model. The influence of the diffusion in the inert part of the catalyst on the bulk concentrations becomes nonnegligible only when the external liquid volume (out of the catalyst) is reduced.

The transient evolution of the concentration profiles in the pores show that hydrogen concentration reaches its steady state within a few seconds, while the evolution of the organic concentration profiles is slower.

Furthermore, the reaction rate has been found to be only affected by the hydrogen diffusion. The diffusion of organics can control the reaction rate only for low values of organic concentration and higher pressure in hydrogen.

Keywords: Three phase hydrogenation; Pore diffusion; Transient diffusion; Non-homogeneous activity; Concentration profiles

1. Introduction

In order to calculate catalyst effectiveness factors during three-phase batch experiments, most authors write steady state equations for the diffusion–reaction model, assuming that the dynamics of pore diffusion is very fast compared to the reaction kinetics. Futhermore, in the case of successive hydrogenation reactions, only the diffusion of hydrogen in the catalyst pores is considered, and not that of the organic reactants.

To determine the role of intraparticle mass transfer for the palladium-catalyzed hydrogenation of methyl linoleate, Tsuto et al. [1] suggested to account for the diffusion of organics, but they wrote steady state diffusion equations. For the hydrogenation of 2,4-dinitrotoluene over a shell Pd/Al_2O_3 catalyst, Molga et al. [2] used a generalized formula for the global effectiveness factor, assuming that only the internal diffusion of hydrogen controlled the apparent reaction rates and that the steady state was reached.

In the case of the hydrogenation of alkylbenzenes, Toppinen et al. [3] investigated the dynamics of the diffusion of the different reactants inside the pores of

*Corresponding author.

0920-5861/99/$ – see front matter
PII: S0920-5861(98)00369-1

the catalyst, but they observed that both organic and hydrogen concentration profiles in the pellet reach their steady state within a few seconds, which is a very short time compared to the timescale of reaction experiments. They also showed that the reaction rate was influenced by the diffusion of hydrogen at high concentration of organics, but that the diffusion of organics began to affect the reaction rate when the concentration in organics has decreased significantly.

The aim of our work is thus to examine in more details the time evolution of concentration profiles inside a catalyst pellet in the case of a three-phase consecutive hydrogenation reaction: the hydrogenation of 1,5,9-cyclododecatriene (CDT) on a 0.5% Pd/Al_2O_3 shell catalyst.

We have also investigated the respective role of hydrogen and organics in the diffusion limitations.

2. Experimental determination of kinetics

The experiments were performed by Stüber et al. [4] and more details can be found in the related paper.

Catalytic hydrogenations were run in a stirred autoclave at different pressures (0.15–1.2 MPa) and temperatures (413–453 K).

Two catalyst particle sizes were used: alumina cylindrical pellets of 3.1 mm diameter impregnated with Pd to a depth of 250 μm (Degussa, E263P/D, 0.5% Pd) and also crushed pellets of mean diameter less than 10 μm in order to determine the intrinsic reaction kinetics.

The experiments were carried out in a semibatch mode with pure CDT (250 g). H_2 was fed continuously to the reactor to maintain a constant pressure. In the case of pellets, 10 g of catalyst was used. Liquid samples were analyzed by a HP 5890 gas chromatograph equipped with a HP-FFAP capillary column.

The products of the reaction are respectively: cyclododecadiene (CDD), cyclododecene (CDE) and cyclododecane (CDA). A simplified scheme for the reaction may be written as follows:

$$\underset{T}{CDT} \xrightarrow[r_1]{H_2} \underset{D}{CDD} \xrightarrow[r_2]{H_2} \underset{E}{CDE} \xrightarrow[r_3]{H_2} \underset{A}{CDA} \quad (1)$$

For the intrinsic kinetics, a Eley–Rideal model was selected.

$$r_i = \frac{m_{Pd} k_i K_j C_j p_{H_2}^{\alpha_i}}{1 + \sum_{j=1}^{3} K_j C_j}, \quad (2)$$

where i is the reaction number, and j is the component number (j=1: CDT, 2: CDD, 3: CDE).

The Arrhenius law defines the rate constants k_i and adsorption constants K_j:

$$k_i = k_{i,0} \exp(-E_i/RT) \quad \text{and} \quad K_j = K_{j,0} \exp(-A_j/RT).$$

The values of kinetic parameters for powder obtained by an optimization procedure for the operating conditions are mentioned in Table 1 [5].

3. Pseudo-steady state and dynamic diffusion–reaction models

Three models were considered: a quasi-steady state model (I), a dynamic model accounting only for the active layer of the catalyst (II), and a dynamic model taking also into account the inert part of the particles (III).

3.1. Model I: quasi-steady state approach

This model is based on the following assumptions:

1. The dynamics of pore diffusion is very fast compared to the reaction kinetics.

Table 1
Kinetic parameters for powder

Frequency factor ($kmol/(m_L^3\ s\ MPa^{\alpha}\ kg_{Pd})$)	Activation energy (kJ/mol)	Frequency factor for adsorption ($m_L^3/kmol$)	Heat of adsorption (kJ/mol)
$k_{1,0}=14.22\times10^7$, $\alpha_1=1$	$E_1=40\times10^3$	$K_{CDT,0}=38.36$	$A_{CDT}=14\times10^3$
$k_{2,0}=16.42\times10^7$, $\alpha_2=1$	$E_2=40\times10^3$	$K_{CDD,0}=15.74$	$A_{CDD}=14\times10^3$
$k_{3,0}=1.81\times10^7$, $\alpha_3=1.36$	$E_3=3.5\times10^3$	$K_{CDE,0}=10.0$	$A_{CDE}=14\times10^3$

2. The depth of the active layer is much smaller than the pellet diameter leading to a slab model with a penetration length δ.
3. External mass transfer limitation is negligible (intense mechanical stirring).
4. The pellet is assumed to be isothermal.

In these conditions the mass balances in the active layer can be written:

$$De_T\left(\frac{\partial^2 C_T}{\partial x^2}\right) - R_1 = 0, \quad De_D\left(\frac{\partial^2 C_D}{\partial x^2}\right) - R_2 + R_1 = 0, \qquad 0 < x < \delta,$$

$$De_E\left(\frac{\partial^2 C_E}{\partial x^2}\right) - R_3 + R_2 = 0, \quad De_H\left(\frac{\partial^2 C_H}{\partial x^2}\right) - (R_1 + R_2 + R_3) = 0, \tag{3}$$

where R_i is the reaction rate per unit volume of the catalyst layer, and De_j is the effective diffusivity of component j.

Since the external mass transfer resistance is negligible, the boundary conditions at the surface of the catalyst are

$$C_{j|_{x=\delta}} = C_{L,j}, \quad j = T, D, E, H \tag{4}$$

with $C_{L,j}$ the bulk concentration of component j, given by

$$V_L \frac{dC_{L,j}}{dt} = -\frac{De_j \times m_{cat}}{\delta \times \rho_P} \times \frac{V_a}{V_P} \frac{\partial C_j}{\partial x}\Big|_{x=\delta}$$

for $j = T, D, E$.

Due to continuous feed of hydrogen and intense stirring, hydrogen concentration in the liquid bulk $C_{L,H}$ is constant and equal to the solubility.

At the limit between the alumina support and the active layer, concentration gradients are equal to zero because of the symmetry condition at the center of the pellet and flux conservation in the inactive support.

On a pratical point of view this model was simulated by using a dynamic diffusion–reaction model and multiplying time derivatives by a factor 10^{-8}. This leads in fact to a pseudo-steady state model.

3.2. Model II: dynamic model of the active layer

With the last three assumptions of model I, the mass balances in the active layer are written as follows:

$$\epsilon \frac{\partial C_j}{\partial t} = De_j\left(\frac{\partial^2 C_j}{\partial x^2}\right) + \sum_i \pm R_i(C_j), \quad 0 < x < \delta. \tag{5}$$

The same boundary conditions are considered, in particular a concentration gradient equal to zero at the interface with the alumina support since only the dynamics of the layer is examined.

$$\forall t,\ x = \delta, \quad C_j = C_{L,j},$$

$$\forall t,\ x = 0, \quad \frac{\partial C_j}{\partial x} = 0. \tag{6}$$

In fact, the inert support is described here as if it was nonporous. The active layer is initially filled with CDT.

3.3. Model III: dynamics of the whole pellet

In this model, the inactive part of the catalyst is taken into account for the isothermal pellet leading to

$$\epsilon \frac{\partial C'_j}{\partial t} = De_j\left(\frac{\partial^2 C'_j}{\partial r^2} + \frac{1}{r}\frac{\partial C'_j}{\partial r}\right), \qquad 0 < r < r_P - \delta,\ j = T, D, E, H \tag{7}$$

in the inactive part of the catalyst.

$$\epsilon \frac{\partial C_j}{\partial t} = De_j\left(\frac{\partial^2 C_j}{\partial r^2} + \frac{1}{r}\frac{\partial C_j}{\partial r}\right) + \sum_i \pm R_i(C_j), \qquad r_P - \delta < r < r_p$$

in the active layer with the following boundary conditions:

$$\forall t, r = 0, \quad \frac{\partial Cj'}{\partial r} = 0 \quad \text{(condition for symmetry)}$$

$$\forall t, r = r_P - \delta, \quad \frac{\partial C_j}{\partial r} = \frac{\partial C'_j}{\partial r}, \quad C_j = C'_j, \tag{8}$$

$$\forall t, r = r_P \quad C_j = C_{L,j} \quad \text{(negligible external mass transfer resistance)}$$

with

$$V_L \frac{dC_{L,j}}{dt} = -\frac{De_j \times m_{cat}}{\delta \times \rho_P} \times \frac{V_a}{V_P} \frac{\partial C_j}{\partial r}\Big|_{r=r_P}$$

for $j = T, D, E$.

The catalyst is assumed to be initially filled with CDT and the bulk hydrogen concentration is constant.

3.4. Model parameters

The effective diffusivity De_j is obtained from the molecular diffusivity by $De_j = (\epsilon/\tau)Dm_j$ with ϵ the porosity (ϵ=0.45) and τ the tortuosity factor (τ=7.2) of the catalyst particles.

The active layer above and below the cylindrical pellet is included in the calculation of the total volume of the layer. This leads to consider a pellet longer than in reality.

3.5. Numerical treatment

The proposed models lead to partial differential equation (PDE) systems. They are solved by the method of lines: spatial derivatives are discretized using central difference formulas.

The resultant ODE systems are solved by a DAE approach using the software RESEDA [6]. This ODE/DAE integrator is originally based on a modified version of the LSODI package initially developed by Hindmarsh [7] and based on Gear method. It has been improved for 10 years in robustness and reliability in order to solve problems typically encountered in the chemical engineering field in which numerical characteristics are rapid transient phenomena, stiffness, large scale systems, high nonlinearity, time and state events, external and intrinsic discontinuities.

For model II, 50 points of discretization were chosen, with 20 for a sub-discretization near the liquid interface. For model III, 81 points were used (50 points for a sub-discretization near the liquid interface). Effectiveness factors are calculated by integrating the rate profiles in the active layer, using the trapezoidal rule.

4. Results and discussion

4.1. Pseudo-steady state approach (model I)

To describe the semibatch experiments of the catalytic hydrogenation of cyclododecatriene, a pseudo-steady state model (derivated from model II) was

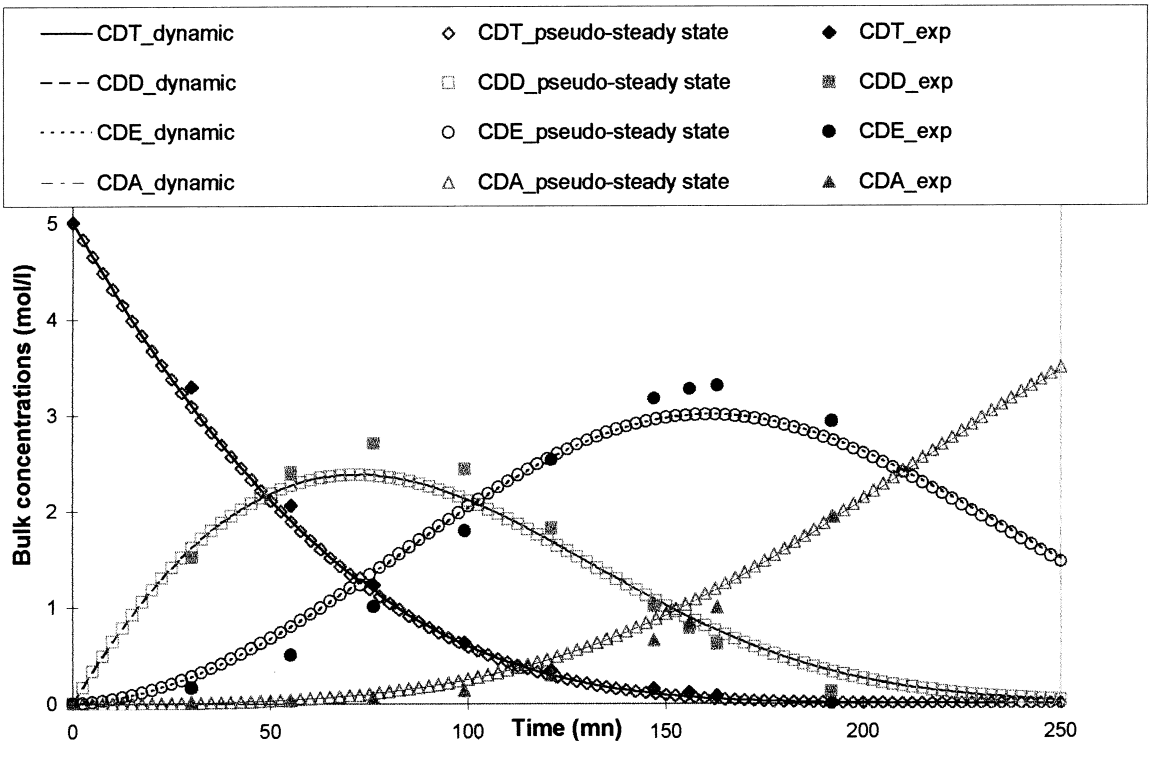

Fig. 1. Predicted and experimental bulk concentrations of hydrocarbons for the models of the active layer (T=433 K, P_{H_2}=1.2 MPa).

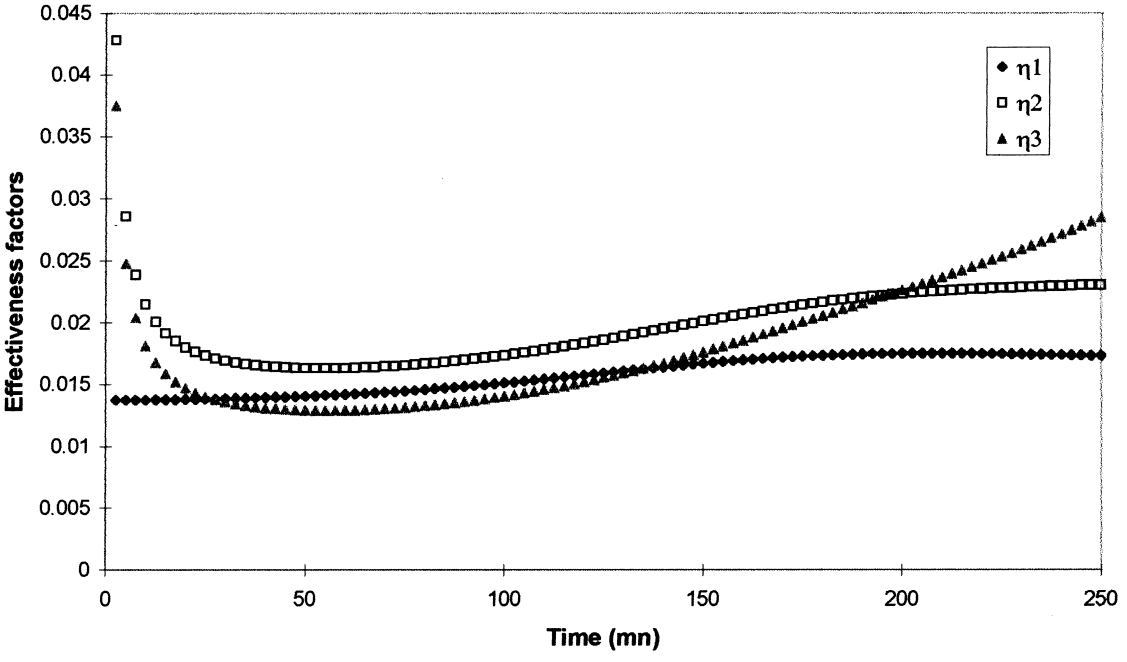

Fig. 2. Effectiveness factors predicted by the pseudo-steady state model of the active layer (T=433 K, P_{H_2}=1.2 MPa).

applied at first; the bulk concentration profiles were calculated versus time and compared to the experimental values. As shown in Fig. 1, the concentrations predicted with this model are in good agreement with the experimental data.

The effectiveness factors obtained for the three reactions have an order of 10^{-2} and increase with time as it was experimentally observed [5] (cf. Fig. 2).

4.2. Dynamic diffusion–reaction model of the active layer (model II)

In this model, the inert support is considered as if it was nonporous, and only profiles in the active layer are presented here.

4.2.1. Preliminary simulations

This model was assessed with a first-order reaction since the calculated concentrations could be compared to analytical expressions:

$$\eta(t) = \frac{\mathrm{th}\Lambda}{\Lambda} - 2\sum_{m=0}^{\infty} \frac{\exp(-[\Lambda^2 + (m+0.5)^2\pi^2]T')}{\Lambda^2 + (m+0.5)^2\pi^2}$$

(see [8])with

$$\Lambda = \delta\sqrt{\frac{k}{D\mathrm{e}}}\ (\text{Thiele modulus}) \quad \text{and} \quad T' = \frac{D\mathrm{e} \times t}{\delta^2\epsilon}. \tag{9}$$

Two assumptions have been formulated for the analytical resolution.

1. The active layer is initially filled with an inert component.
2. The surface of the layer is maintained at a constant reactant concentration C_S.

For different values of the Thiele modulus, the numerical model and the analytical solution have been found to perfectly give the same evolution of the dynamic effectiveness factor.

4.2.2. Catalytic hydrogenation of CDT: dynamic behavior of the active layer

In order to investigate the transients of the concentration profiles in the catalyst layer during the hydrogenation of CDT, a simulation assuming constant bulk

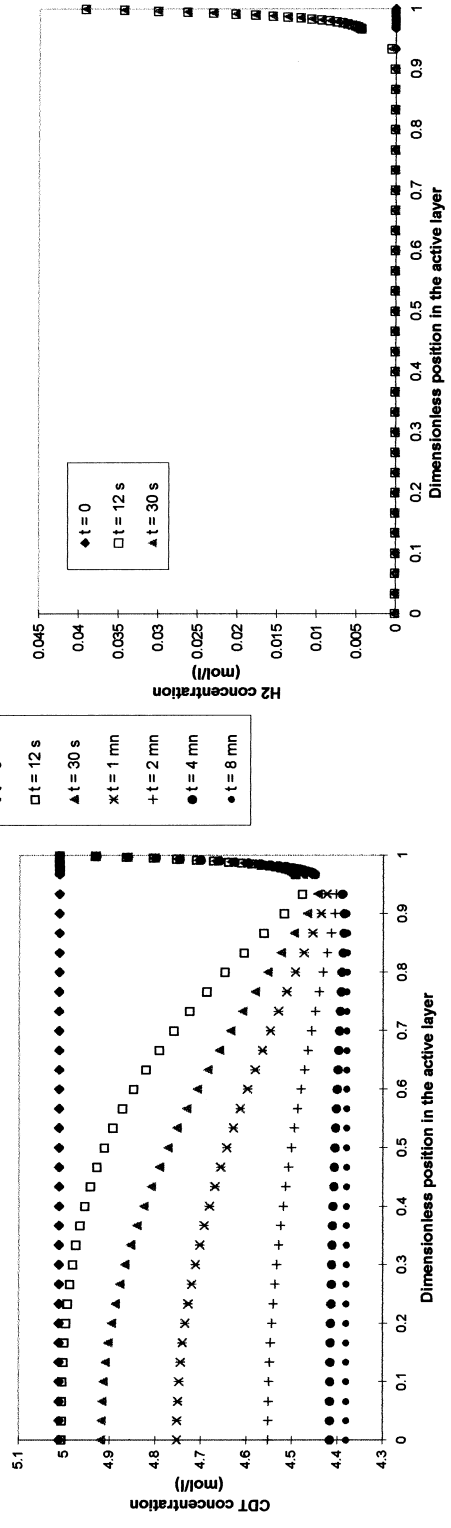

Fig. 3. Development of concentration profiles for the dynamic model of the active layer (T=433 K, P_{H_2}=1.2 MPa): (a) CDT; (b) H_2.

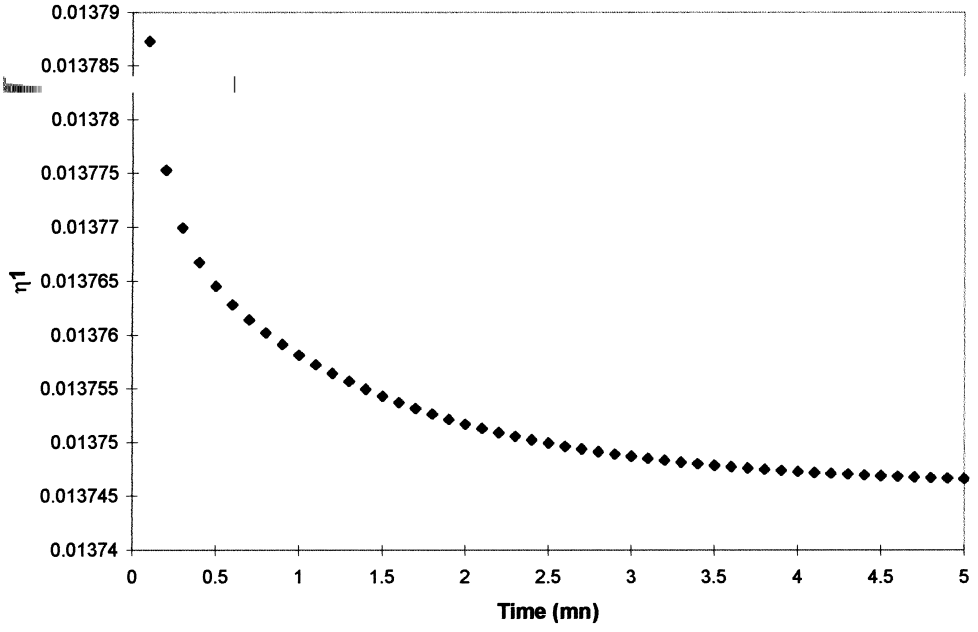

Fig. 4. Effectiveness factor evolution for the dynamic model of the active layer (T=433 K, P_{H_2}=1.2 MPa).

concentrations (equal to the liquid phase concentrations at t=0) was achieved.

The system of equations involve the differential system (5), and the boundary condition: $C_{L,j}=C_{L,j0}$.

Figs. 3 and 4 show that steady state values are reached almost immediately for the hydrogen concentration and for the effectiveness factor (η_1, but that the evolution of the organic concentration profiles is slower. The influence of various parameters has been studied: the most significant one is the hydrocarbon effective diffusivities which are very low in our case (10^{-10} m^2/s). By multiplying them by 10, the steady state for the organic profiles would be reached in less than 1 min.

In order to study the respective role of hydrogen and organic diffusion limitations, a simulation with hydrogen and organic concentrations of the same order has been achieved: the pressure in hydrogen has been multiplied by a factor 10, while organic concentrations have been divided by the same factor. Whereas only hydrogen controlled the kinetics in the conditions of the experiments, Fig. 5(a) and (b) show that in this case the reaction rates are no longer affected by the hydrogen concentration profile, but by the organic diffusion: indeed the CDT concentration profile tends toward zero in the most part of the layer when steady state conditions are reached (Fig. 5(b)). In both figures, steady state values are obtained within less than 2 min.

4.2.3. *Catalytic hydrogenation of CDT: semibatch reaction*

The dynamic model II was also applied to the semibatch catalytic hydrogenation of cyclododecatriene. Fig. 1 shows the same bulk concentration evolution as that obtained with the pseudo-steady state model, but the hydrocarbon concentration profiles in the pores are slightly dependent on the model (cf. Fig. 6(a)). However, internal hydrogen concentration profiles are similar in both cases: the concentration is equal to zero in the most part of the layer (cf. Fig. 6(b)). This explains why the effectiveness factors are the same with the two models, despite different internal hydrocarbon concentrations.

4.3. *Dynamic diffusion–reaction model in the whole pellet (model III)*

In order to describe more precisely the concentration profiles inside the pellet, the dynamic model was

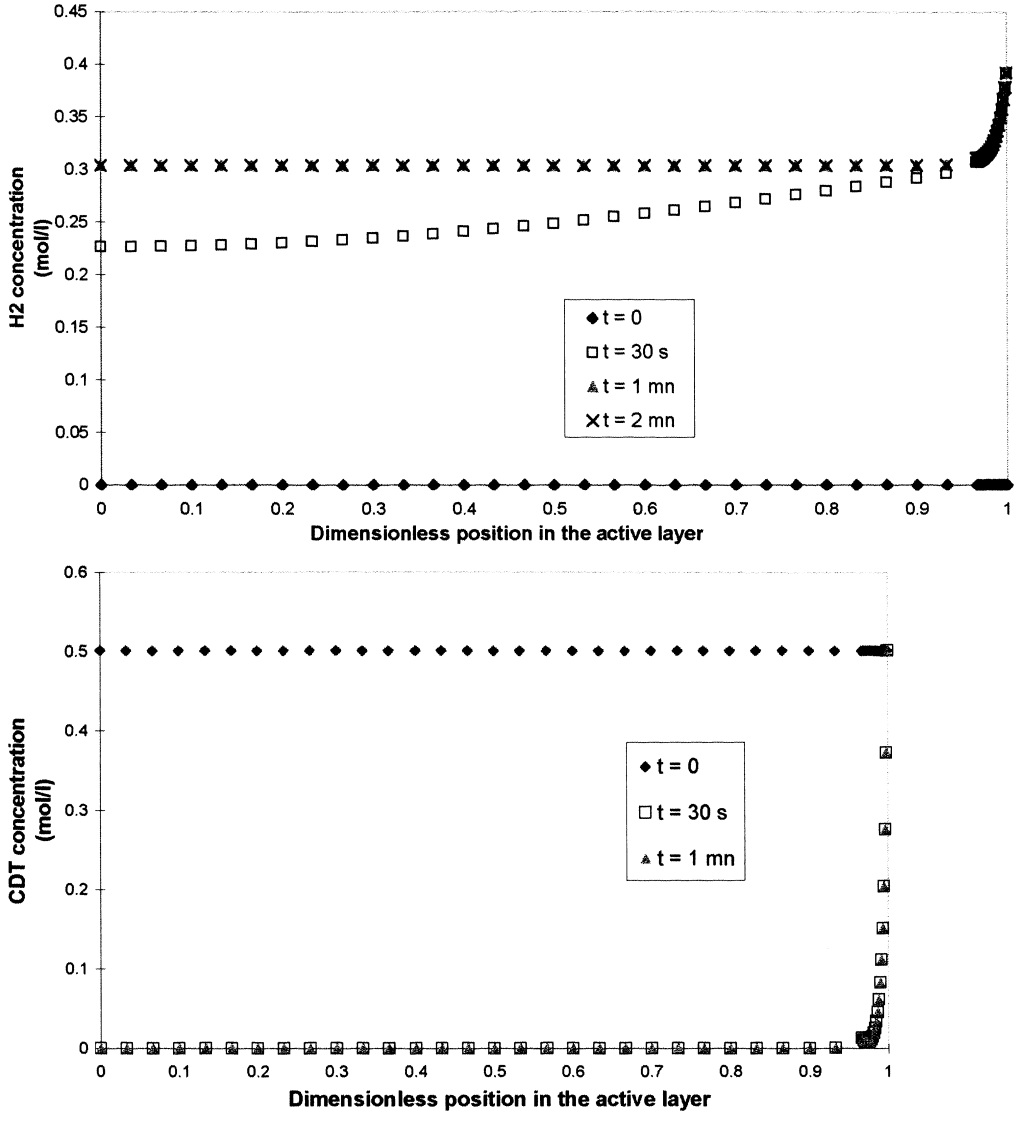

Fig. 5. Development of concentration profiles for the dynamic model of the active layer for a low CDT concentration and a high pressure in H_2: (a) CDT; (b) H_2.

improved by taking into account the diffusion of the reactants in the inactive part of the catalyst (the gradient at the limit between the active layer and the alumina support is no longer assumed to be equal to zero). In fact, the volume in the inactive part of the pellet acts as a supply of reactants, becoming non-negligible when the volume of liquid (out of the catalyst) is reduced.

4.3.1. *Catalytic hydrogenation of CDT: study of the semibatch reaction*

This complete model was applied to the semibatch catalytic hydrogenation of cyclododecatriene: the model predictions for the bulk concentrations fit well the experimental data, but not clearly better than the simplified pseudo-steady state model. In fact the time evolution of the bulk concentrations

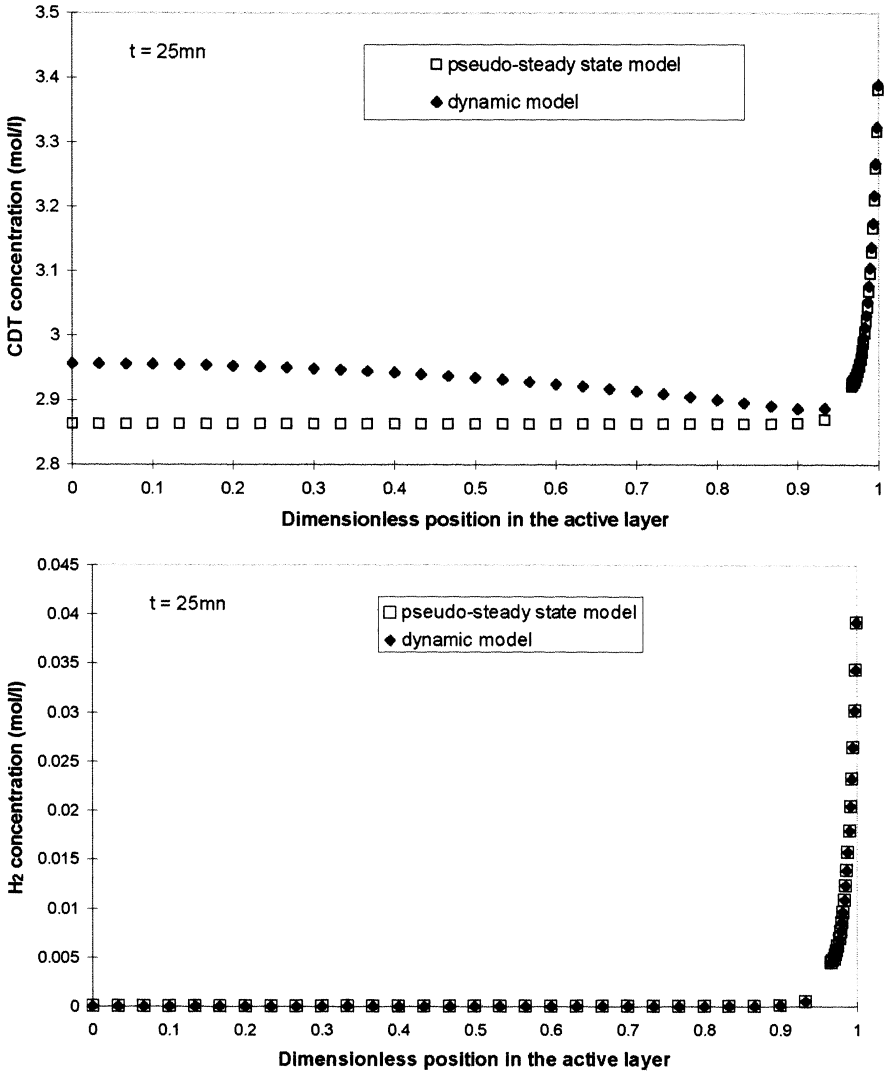

Fig. 6. Concentration profiles in the active layer for the pseudo-steady state and the dynamic model (T=433 K, P_{H_2}=1.2 MPa): (a) CDT; (b) H_2.

is not influenced by the unsteady diffusion (cf. Fig. 7). However, hydrocarbon internal profiles are very much dependent on the model. Fig. 8(a) shows the CDT concentration profile in the pellet: after a steep decrease of concentration at the pellet surface, due to the disparition of H_2, the CDT concentration increases again in the pellet due to the slow diffusion from the inert porous volume.

4.3.2. *Catalytic hydrogenation of CDT: external liquid volume divided by a factor 50*

Model III was then run for conditions close to those of a fixed bed: an external liquid volume divided by 50. In this case, the liquid volume in the pores is no longer negligible compared to the bulk liquid volume. The dynamic and the pseudo-steady state models lead now to distinct bulk concentration curves (cf. Fig. 9): the diffusion of the different species in the inert part of

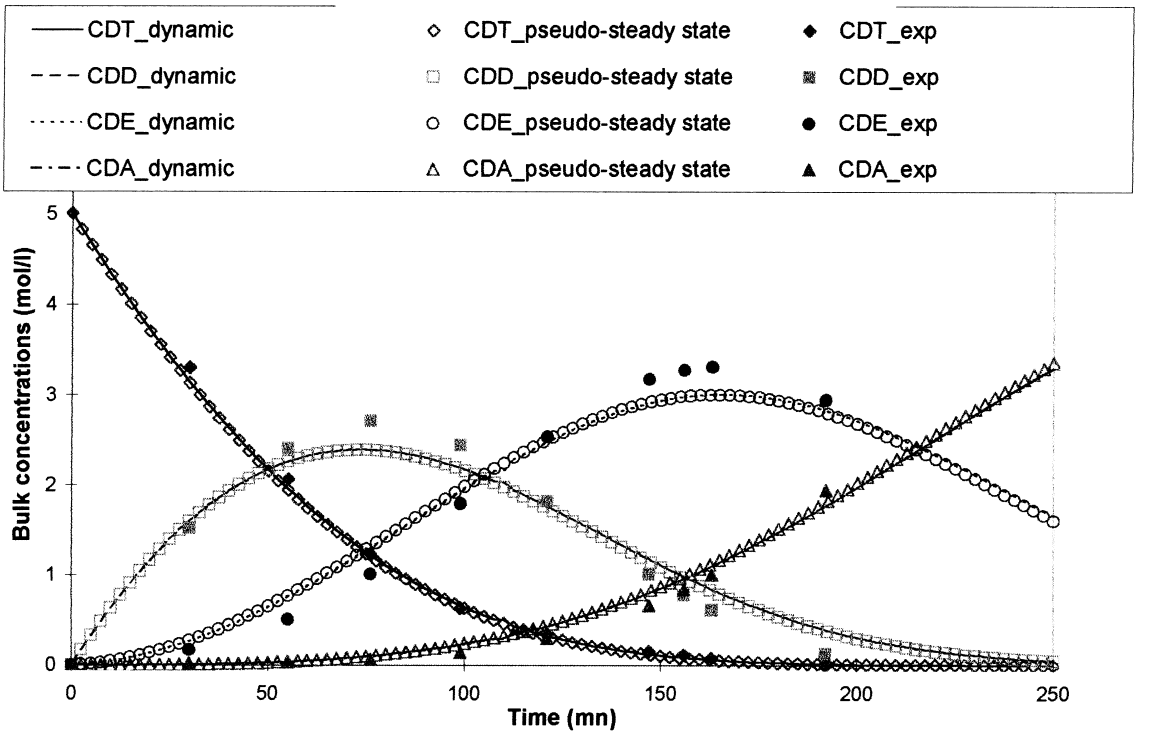

Fig. 7. Predicted and experimental bluk concentrations of hydrocarbons for the pseudo-steady state and the dynamic models in the whole pellet (T=433 K, P_{H_2}=1.2 MPa).

the pellet induces a delay in these curves. However, the differences are not very significant and the values of the maxima of concentrations in CDE are quite the same.

The transient internal concentration profile of CDT calculated for the same extent of the reactions as in Fig. 8(a) is yet very different (cf. Fig. 10), showing a very slow diffusion of CDT out of the core of the pellet to the reaction zone. Even if the degrees of advancement have the same values in Fig. 8(a) and Fig. 10, the diffusional process does not play the same role. As shown in Fig. 10, the pores are still filled with CDT, whereas a high amount of this reactant has already been consumed in the liquid bulk.

5. Conclusion

Different models for the calculation of the effectiveness factors and the concentration profiles in the pores of a shell catalyst have been compared.

For the catalytic hydrogenation of cyclododecatriene, all the models lead to a good (and the same) prediction of the bulk concentration–time curves. However they predict different organic profiles in the pores. Here the kinetics is mainly limited by the diffusion of hydrogen. That explains why the bulk concentration evolution is quite the same, even if the organic concentration profiles in the pellet are very different. The diffusion of organics can become limiting only for low values of the organic concentrations and higher pressures in hydrogen.

The description of the diffusion in the inert part of the particles shows an influence on the bulk concentrations, only when the liquid volume is reduced.

6. Nomenclature

C_j concentration of component j in the active layer $(\mathrm{kmol/m_L^3})$

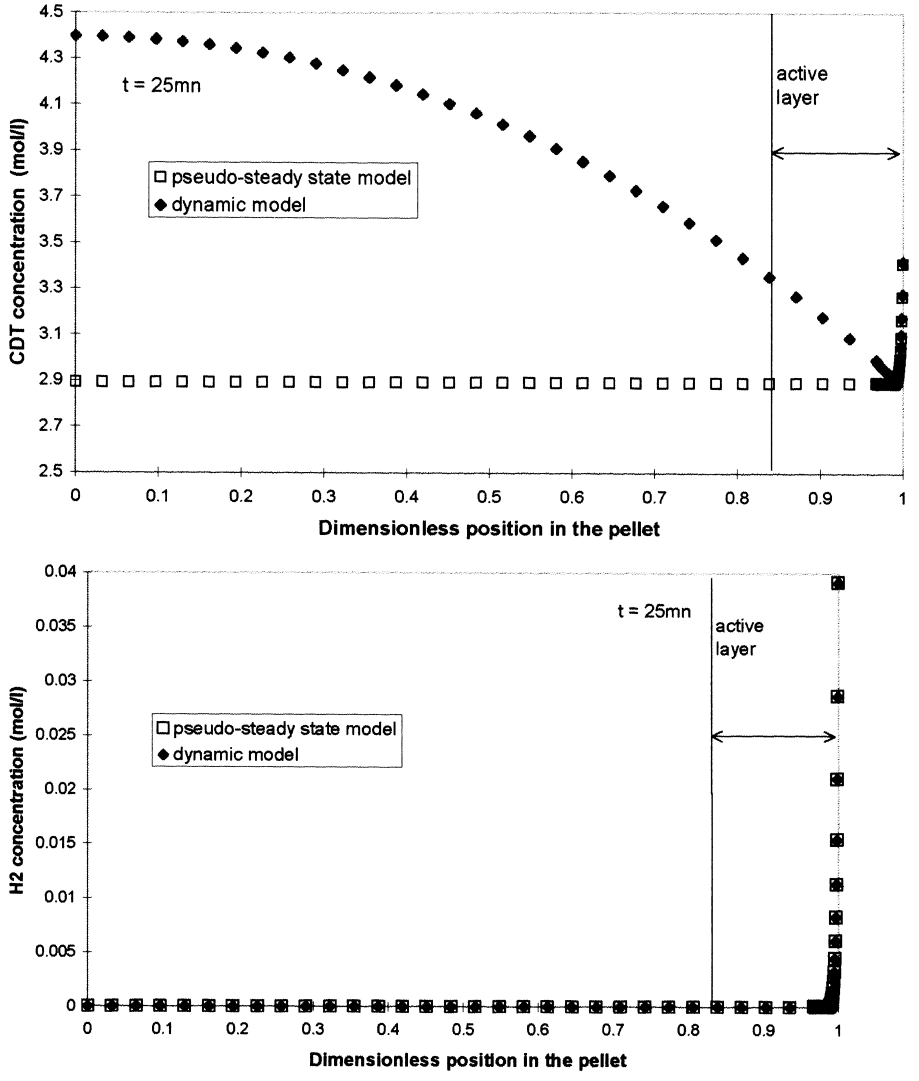

Fig. 8. Concentration profiles in the whole pellet for the pseudo-steady state and the dynamic models (T=433 K, P_{H_2}=1.2 MPa): (a) CDT; (b) H_2.

C'_j concentration of component j in the inactive part of the catalyst (kmol/m^3_L)
$C_{L,j}$ bulk concentration of component j (kmol/m^3_L)
$C_{L,j0}$ initial bulk concentration of component j (kmol/m^3_L)
D_e effective pore diffusivity (m^2/s)
D_m molecular diffusivity (m^2/s)
k_i kinetic constant of reaction i (kmol/(m^3_L s MPa^{α} kg_{Pd}))
K_j adsorption constant of component j (m^3_L/kmol)
m_{cat} weight of catalyst pellet (kg)
m_{Pd} weight of active catalyst (Pd) (kg)
p_{H_2} pressure of hydrogen (MPa)
r_i reaction rate of reaction i (kmol/m^3_L/s)
R_i reaction rate per unit volume of active layer (kmol/$m^3_{active\ layer}$/s)
r_P pellet radius (m)

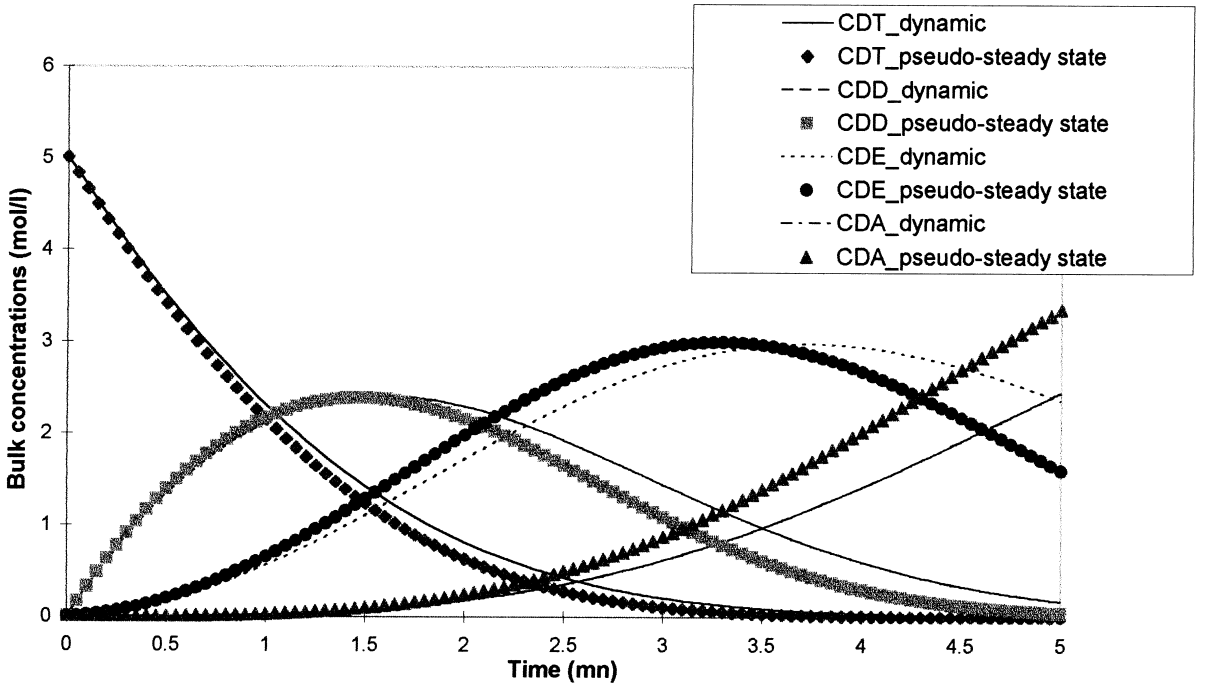

Fig. 9. Predicted and experimental bulk concentrations of hydrocarbons for the pseudo-steady state and the dynamic models in the whole pellet – external liquid volume divided by 50 (T=433 K, P_{H_2}=1.2 MPa).

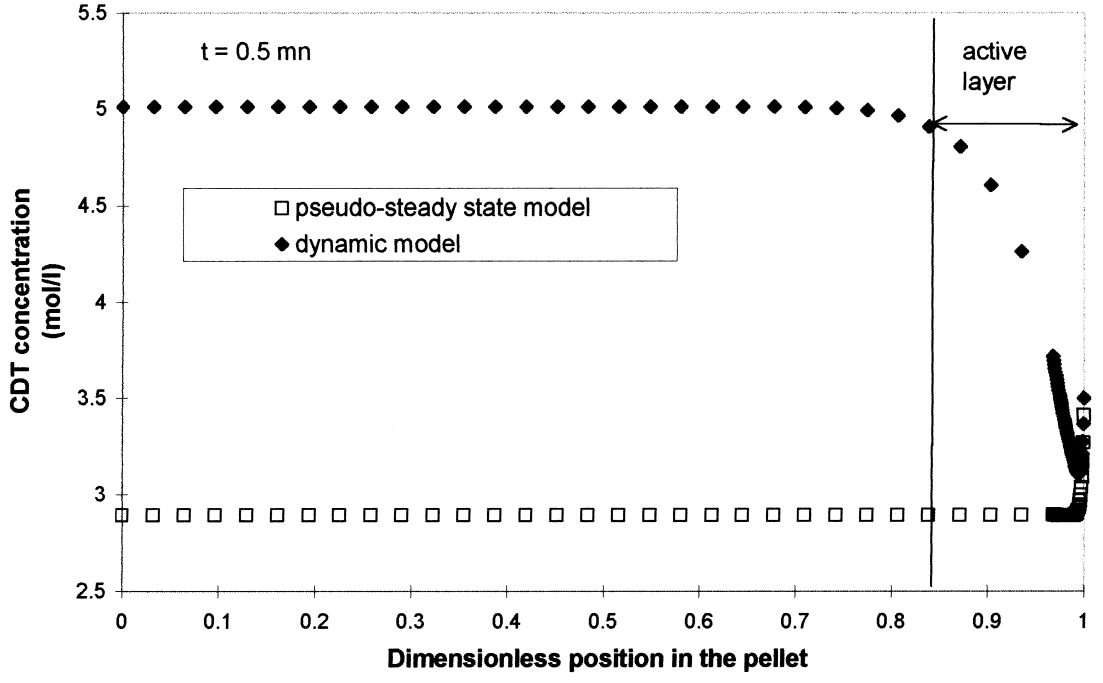

Fig. 10. CDT concentration profiles in the whole pellet for the pseudo-steady and the dynamic models – external liquid volume divided by 50 (T=433 K, P_{H_2}=1.2 MPa).

V volume (m^3)

V_a volume of the active layer on a pellet (m^3)
V_P volume of a pellet (m^3)

Greek symbols

δ penetration depth of the active layer (m)
ϵ porosity of the pellet
η_i effectiveness factor of reaction i
ρ_P density of catalyst particles (kg/m^3)
τ tortuosity factor
Λ Thiele modulus

Subscripts and abbreviations

A cyclododecane
D cyclododecadiene
E cyclododecene
T cyclododecatriene
H_2 hydrogen
i number of reaction
j number of reacting species
L liquid bulk

Acknowledgements

The authors wish to thank IFCPAR (Indo-French Center for the Promotion of Advanced Research) for financial support.

References

[1] K. Tsuto, P. Harriott, K.B. Bischoff, Ind. Eng. Chem. Fundam. 17(3) (1978) 199.
[2] E.J. Molga, K.R. Westerterp, Chem. Eng. Sci. 47(7) (1992) 1733.
[3] S. Toppinen, T.K. Rantakylä, T. Salmi, J. Aittamaa, Ind. Eng. Chem. Res. 35 (1996) 1824.
[4] F. Stüber, M. Benaissa, H. Delmas, Catal. Today 24 (1995) 95.
[5] M. Benaissa, Ph.D Thesis, INP, Toulouse, 1994.
[6] J.M. Le Lann, Internal Report, User Manual, 1996.
[7] A.C. Hindmarsh, ACM SIGMUN Newsletter 15 (1980) 10.
[8] J.V. Villadsen, W.E. Stewart, Chem. Eng. Sci. 22 (1967) 1483.